SCIENTIFIC PAPER

GAS-LIQUID DISPERSION AGITATED BY CLOSED TURBINE TYPE IMPELLER

Masanori Yoshida*, Toshiki Kosaka, Yoshiki Mukai, Koichi Nakahara, Reno Kiyota

Department of Applied Sciences, Muroran Institute of Technology, Muroran, Japan

https://doi.org/10.2298/CICEQ240411027Y

Received 11.4.2024.

Revised 20.6.2024.

Accepted 16.7.2024.

---

* Correspondence: M. Yoshida, Department of Applied Sciences, Muroran Institute of Technology, 27-1, Mizumotocho, Muroran 050-8585, Japan.

Tel: +81-143-46-5761

E-mail: myoshida@mmm.muroran-it.ac.jp

Abstract

Gas-liquid agitation by a turbine type impeller having shrouds structurally (closed disk turbine impeller, CDT) was studied by examination of the flow behavior of gas-liquid mixture in the impeller region, with energy consideration based on the impeller power characteristics in the gassed liquid. The way in formation of the gas cavities and dispersion as the gas bubbles using the CDT differed from that using a conventional disk turbine impeller (open impeller, ODT). The difference in relative power consumption, i.e., ratio of gassed to ungassed power consumption, between the CDT and ODT was related to the configurations of the gas cavities.

Key words: gas-liquid agitation, closed turbine type impeller, gas cavity, impeller region, power characteristics.

Article Highlights

- A turbine type impeller having shrouds (closed impeller, CI) is applied to gas-liquid agitation
- Formation of the gas cavities and dispersion as the gas bubbles through the CI are characterized
- The power consumption of CI in operation handling gas-liquid dispersion is assessed

INTRODUCTION

A vessel agitated by a mechanically rotating impeller is a typical apparatus to perform chemical processes involving the operation of dispersions such as gas-liquid mixtures. The impeller improves the gas-liquid contact, dispersing sparged gas as gas bubbles, thereby enhancing phenomena of reaction and mass transfer between the gas and liquid phase. A shearing deformation action is desired for the impeller to generate the gas bubbles in the liquid in turbulent flow. Preferably, a disk turbine impeller with six flat blades has been employed because of its relatively strong action. However, the flat bladed turbine type impellers have an important weakness when used for gas-liquid agitation [1]. Studies [2–8] have emphasized the variable configurations of gas cavities forming behind the impeller blades. That variation affects the capacity for the impeller to handle the gas or the power inputted by the impeller. Information about impellers improved in use for gas-liquid agitation is available in the literatures [9-12]. One proposal is a disk turbine impeller with six hollow (concave) blades [13,14]. The concave bladed turbine impeller had an enhanced gas-handling capacity. Additionally, the power fall under gassing was alleviated, compared with that for the flat bladed turbine impeller. These improved performances were attributed to reduced formation of the gas cavities [15-18]. Because the gas cavities play a role as generating the gas bubbles, their formation should be evaluated for an effectiveness rather than the result of reduction.

Previously, we proposed a design of agitation impeller with alteration of a conventional turbine type impeller [19]. A concept of the alterative design was for the impeller blades to transmit energy fully. This impeller, which has shrouds structurally, was named a “closed disk turbine impeller (CDT)” in contrast with a conventional “open disk turbine impeller (ODT)”. In a baffled vessel agitated by the CDT, the internal liquid flow in the impeller rotation region was examined to be analyzed for energy consideration [19]. Comparison of the power characteristics between the CDT and ODT demonstrated an increased transmission of energy and its possibly uniformized dissipation. The CDT has higher efficiency of energy transmission. Additionally, the centrifugal action with the CDT is advantageous to produce the radial flow with a high level of turbulence. Accordingly, a successful performance is expected for the CDT agitating mixtures in dispersion systems.

In the present work, the closed disk turbine impeller (CDT) was applied to gas-liquid agitation. Visual observation using a video camera was made for the region of impeller rotation with gas sparging into liquid. The flow behavior of gas-liquid mixture for the CDT was investigated and characterized with emphasis on formation of the gas cavities and dispersion as the gas bubbles, by contrast with that for the open disk turbine impeller (ODT). The power characteristics of CDT in the gassed liquid were evaluated in relation to operation of the gas-liquid dispersion.

EXPERIMENTAL

An experimental setup was constituted with a standard agitation vessel and a gassing system. A fully baffled cylindrical vessel with a flat base made of transparent acrylic resin (300 mm inner diameter, D_t) was used. Four vertical baffles with a width of $D_t/10$ were fitted along the internal wall of the vessel, spaced equally around the circumference. The ungassed liquid depth was maintained at D_t, i.e., 300 mm. Figure 1 shows the closed impeller designs [19].

[Fig. 1 insert position]

Its diameter, D_i, was 150 mm ($=D_t/2$). An open impeller of the equal size in D_i was used for comparison. The respective impellers were set at a height of $D_t/3$ from the vessel bottom. The impeller rotation rate, N_r, was varied from 50 to 200 rpm. A single hole nozzle of 5.0 mm inner diameter was used for air sparging. The volumetric gas flow rate, Q, was varied from 5 to 70 L min^{-1} for the superficial gas velocity, V_s, of 0.12-1.65 cm s^{-1}.

Visualization of the gas behavior as it is sparged into the liquid within the vessel was done based on views from the bottom and the front. In the bottom view, the conditions were observed for the impeller to capture the gas and to generate gas bubbles. In the front view, the conditions of the bubble dispersion were observed in the bulk liquid. The gas behaviors were recorded as continuous images using a video camera with a 1000 fps frame rate. For the liquid flows produced by the respective impellers, the results measured with PTV, which were presented in the earlier reports [19,20], were used as references. The impeller power consumption was determined by measuring the torque with strain gauges fitted onto the shaft [19,20].

RESULTS AND DISCUSSION

Flow behavior of gas-liquid mixture

Figure 2 depicts the region where the impeller rotates at the rate, N_r, of 140 rpm under the condition of gassing in the superficial gas velocity, V_s, of 0.12 cm s^{-1}.

[Fig. 2 insert position]

In the figures, (a) is for the open impeller (ODT); (b) is for the closed impeller (CDT). The aeration number is defined as follows:

$$N_a = \frac{Q}{N_r {D_i}^3} \tag{1}$$

For its value of 0.011, the agitation level is evaluated as relatively larger than the aeration level [21]. In the ODT operated under this aeration-agitation rate condition, the vortex cavities [22] remained stable, forming on the rear sides near the upper and lower edges of the impeller blades. The sparged gas was captured steadily by the cavities. The gas bubbles were generated continuously from the end of cavities into the bulk liquid [23]. The upper and lower edges of the CDT blades are shrouded with the doughnut-shaped disks. Therefore, no vortex cavity was observed in the form similar to that forming behind the ODT blades. With use of the CDT, the sparged gas was aggregated as cavities on the rear sides of the impeller blades. Each cavity grew circumferentially long. Generation of the gas bubbles occurred radially around the exit of the impeller rotation region.

For the ODT in such an operational condition, it has been known that the path-line of sparged gas is almost the same as that of liquid in single-phase flow [23]. Figure 3 illustrates a profile of the velocity in single-phase liquid flow [19] superimposed on the image of the impeller handling the gas-liquid mixture.

[Fig. 3 insert position]

The velocity profiles were determined on the different heights of horizontal planes. The figure (a) is for the open impeller (ODT). The profile at the height of 6 mm above the lower blade edge was picked up. The figure shows the vectors for the flow velocity relative to the impeller rotation. As expected for the ODT, the path-line of the sparged gas coincides with that for the liquid flow. In the impeller inside region, the gas behavior and the liquid flow were in common characterized as an intensified stream with radial discharge behind the blade. Outside the impeller, an elongated zone with a larger velocity gradient in the liquid flow was detected, possibly because of a rotation flow in the trailing vortex. A line to characterize such a zone overlapped the trajectory of the gas cavity. The figure (b) is for the closed impeller (CDT). The profile at the height of 2 mm above the lower blade edge was picked up. The CDT had the path-line common to the gas and liquid. For the internal region, the liquid flow was found to be distributed into the front and rear sides between the impeller blades. A line to characterize the distributary was detected. On the line, the gas cavity formed with handling the gas-liquid mixture. Such a flow field appears to be attributable to the flow produced secondarily as a consequence of the shrouding disk fitted to the blade edges.

To observe the efficacy of the shrouding disk, the profile of the circumferential flow velocity was investigated for the single-phase liquid between the blades. Figure 4 shows the circumferential velocities of the inflow (40.0 mm radial position) and outflow (72.5 mm radial position) in the developed view of the faces of the circular cylinders forming in the respective positions, where the flow velocity is relative to the impeller rotation. Plates (a) and (b) in the figure are related respectively to the open impeller (ODT) and the closed impeller (CDT).

[Fig. 4 insert position]

For the ODT, the flows toward the front surface of the blade were observed in most parts of the region. In the CDT, the flows were induced, as caused by the pressure gradient [24,25]. They trended from the front of higher pressure to the back of lower pressure. Such a secondary flow, which was detected in the layer near the inner surface of the shrouding disk, extended axially and covered the entire blade surface. The gas cavity in the gas-liquid system is believed to form in the orientation from higher to lower pressure according to the pressure gradient.

Figure 5 depicts the gassed regions of the ODT (a) and the CDT (b) under the conditions of the impeller rotation rate, N_r, of 140 rpm and the superficial gas velocity, V_s, of 0.47 cm s^{-1}.

[Fig. 5 insert position]

Then, the aeration number, N_a, of 0.042 indicates a relatively increased aeration level [21]. In the ODT, vortex-like cavities clinging to the blades and larger cavities blanketing the blades formed alternately [22]. As compared the image (a) between Figs 2 and 5, generation of the gas bubbles through the large cavities tended to deviate from the radial direction to the circumferential direction. Reduction in gas dispersion was suggested due to formation of the large cavities hindering a part of the radially outward liquid flow [23]. Comparison of the image (b) between Figs 2 and 5 demonstrated with the CDT that the aeration-agitation rate condition exerted a slight effect on formation of the cavities and generation of the gas bubbles: the circumferentially long cavities generated effectively the gas bubbles in a radially outward direction. The dependence of gas dispersion on the operational condition was found to differ between the ODT and CDT. This suggests a difference of centrifugal effect in the gas cavities forming in the respective impellers. As shown in Fig. 4, the circumferential outflow velocity relative to the impeller rotation was smaller overall with the CDT than with the ODT. That is, the CDT produces a flow field rotating with larger absolute velocities, which can lead to a favorable centrifugal effect.

Relation between power consumption and cavity formation

Formation of gas cavities behind the impeller blades and dispersion as gas bubbles within the vessel can affect energy transmission through the impeller [22]. This effect has been assessed in terms of the ratio of gassed power consumption to ungassed one of the impeller, P_{mg}/P_{m0}. Changes in the power consumption are observed with variation of the impeller rotation rate, N_r, under a constant condition of the superficial gas velocity, V_s, or with variation of V_s under a constant condition of N_r. Here, the latter approach was employed. The results were coordinated in terms of the aeration number, N_a. Figure 6 shows the relationships between P_{mg}/P_{m0} and N_a for the ODT and CDT, respectively.

[Fig. 6 insert position]

When the ODT was operated at a lower rotation rate such as 50 rpm, the impeller has ineffectual dispersions according to the flow regime map [21]. Then, the P_{mg}/P_{m0} values close to 1, which indicate a power characteristic unaffected by gassing, can reflect unsatisfactory dispersions. For the CDT operated at the rotation rate of 50 rpm, decreases in P_{mg}/P_{m0} were observed, suggesting some level of successful working of the impeller. With increase of the impeller rotation rate, on the whole, P_{mg}/P_{m0} tended to decrease commonly for the ODT and CDT. The ODT, being operated at a higher rotation rate such as 200 rpm, had larger decreases in P_{mg}/P_{m0} under higher aeration rate conditions, probably because of formation of the large cavities [21]. For the CDT, decreases in P_{mg}/P_{m0} were smaller than those for the ODT, which supports the smaller effect of aeration-agitation rate condition on formation of the cavities. Additionally, as predicted from the images presented in Fig. 7, the impeller region shrouded by the hollow disk can function to capture the sparged gas.

[Fig. 7 insert position]

Increased gas hold-up in the impeller region is regarded as potentially contributing to the power reduction. Overall, the power characteristics of CDT were perceived as stable with variation of the operational conditions. This demonstrates for the CDT the higher efficiency of energy transmission through the impeller and the effective gas-liquid agitation by the impeller for widely various aeration-agitation rates.

Moreover, in order to confirm the effective gas-liquid agitation by the CDT, more quantitative examinations are desired for mass transfer enhancement in terms of the volumetric coefficient, including the gas hold-up and gas bubble diameter.

CONCLUSION

The flow behavior of gas-liquid mixture agitated by the closed disk turbine impeller (CDT) was examined through flow visualization and measurement, in comparison with that agitated by the open disk turbine impeller (ODT). In the CDT, the path-line for the motion was common to the sparged gas and single liquid, as is the case with that for the vortex motion characteristic in the ODT. The cavities forming in the CDT generated the gas bubbles, nearly independent of the aeration-agitation rate condition. The ratio of gassed to ungassed power consumption of the impeller was assessed as a reflection of formation of the gas cavities and dispersion as the gas bubbles. For widely various aeration-agitation rates, energy transmission through the CDT was revealed to be better than that through the ODT forming the large cavities.

Nomenclature

D_i - impeller diameter, mm

D_t - vessel diameter, mm

N_a - aeration number, -

N_r - impeller rotation rate, rpm

P_{m0} - ungassed impeller power consumption, W

P_{mg} - gassed impeller power consumption, W

Q - volumetric gas flow rate, L min^{-1}

V_s - superficial gas velocity, cm s^{-1}

REFERENCES

[1] G.M. Mule, A.A. Kulkarni, Chem. Ind. Dig. July (2015) 58-64. https://www.researchgate.net/publication/358901096

[2] H.R. Lee, Y.J. Huh, C.S. Choi, W.H. Lee, Kor. J. Chem. Eng. 9 (1992) 164-168. https://doi.org/10.1007/BF02705134

[3] V.V. Ranade, V.R. Deshpande, Chem. Eng. Sci. 54 (1999) 2305-2315. https://doi.org/10.1016/S0009-2509(98)00301-7

[4] V.V. Ranade, M. Perrard, C. Xuereb, N. Le Sauze, J. Bertrand, Chem. Eng. Res. Des. 79 (2001) 957-964. https://doi.org/10.1205/02638760152721190

[5] M. Mochizuki, H. Sato, Y. Doida, Y. Saita, T. Amanuma, T. Takahashi, Kagaku Kogaku Ronbunshu 34 (2008) 557-561. https://doi.org/10.1252/kakoronbunshu.34.557

[6] F. Maluta, A. Paglianti, G. Montante, Chem. Eng. Sci. 241 (2021) 116677. https://doi.org/10.1016/j.ces.2021.116677

[7] C. Yang, H. Lu, B. Wang, Z. Xu, B. Liu, Chem. Eng. Sci. 280 (2023) 119058. https://doi.org/10.1016/j.ces.2023.119058

[8] F. Maluta, F. Alberini, A. Paglianti, G. Montante, Chem. Eng. Res. Des. 194 (2023) 582-596. https://doi.org/10.1016/j.cherd.2023.05.006

[9] R. Sardeing, J. Aubin, C. Xuereb, Chem. Eng. Res. Des. 82 (2004) 1589-1596. https://doi.org/10.1205/cerd.82.12.1589.58030

[10] Z. Zheng, D. Sun, J. Li, X. Zhan, M. Gao, Chem. Eng. Res. Des. 130 (2018) 199-207. https://doi.org/10.1016/j.cherd.2017.12.021

[11] D. Gu, Y. Mei, L. Wen, X. Wang, Z. Liu, J. Taiwan Inst. Chem. Eng. 121 (2021) 20-28. https://doi.org/10.1016/j.jtice.2021.03.038

[12] D. Li, W. Chen, Process Saf. Environ. Prot. 158 (2022) 360-373. https://doi.org/10.1016/j.psep.2021.12.019

[13] F. Saito, A.W. Nienow, S. Chatwin, I.P.T. Moore, J. Chem. Eng. Jpn. 25 (1992) 281-287.

https://doi.org/10.1252/jcej.25.281
[14] J. Zhao, Z. Gao, Y. Bao, Chin. J. Chem. Eng. 19 (2011) 232-242. https://doi.org/10.1016/S1004-9541(11)60160-2
[15] B.H. Junker, M. Stanik, C. Barna, P. Salmon, E. Paul, B.C. Buckland, Bioprocess Eng. 18 (1998) 401-412. https://doi.org/10.1007/s004490050463
[16] M. Cooke, P.J. Heggs, Chem. Eng. Sci. 60 (2005) 5529-5543. https://doi.org/10.1016/j.ces.2005.05.018
[17] G. Montante, A. Paglianti, Chem. Eng. J. 279 (2015) 648-658. http://dx.doi.org/10.1016/j.cej.2015.05.058
[18] D. Gu, L. Wen, H. Xu, M. Ye, J. Taiwan Inst. Chem. Eng. 143 (2023) 104688. https://doi.org/10.1016/j.jtice.2023.104688
[19] M. Yoshida, H. Ebina, K. Ishioka, K. Oiso, H. Shirosaki, R. Tateshita, Int. J. Chem. React. Eng. 15 (2017) 20160198. https://doi.org/10.1515/ijcre-2016-0198
[20] M. Yoshida, H. Ebina, H. Shirosaki, K. Ishioka, K. Oiso, Braz. J. Chem. Eng. 32 (2015) 865-873. https://doi.org/10.1590/0104-6632.20150324s00003682
[21] J.C. Middleton, in Mixing in the process industries, N. Harnby, M.F. Edwards, A.W. Nienow Eds., Butterworth-Heinemann, Oxford (1992), pp. 322-363. ISBN-13: 978-0750637602
[22] W. Bruijn, K. van’t Riet, J.M. Smith, Trans. Inst. Chem. Eng. 52 (1974) 88-104. ISSN: 0046-9858
[23] K. van’t Riet, J.M. Smith, Chem. Eng. Sci. 28 (1973) 1031-1037. https://doi.org/10.1016/0009-2509(73)80005-3
[24] K. Brun, R. Kurz, Int. J. Rotating Mach. 1 (2005) 45-52. https://doi.org/10.1155/IJRM.2005.45
[25] C. Wu, K. Pu, C. Li, P. Wu, B. Huang, D. Wu, Energy 246 (2022) 123394. https://doi.org/10.1016/j.energy.2022.123394

Figure Captions

Figure 1. Schematic drawing of a closed impeller (dimensions in mm).

Figure 2. Bottom view of impellers of (a) open and (b) closed type rotating with gassing under lower aeration rate condition.

Figure 3. Gas behavior and liquid flow in regions of (a) open and (b) closed impellers.

Figure 4. Circumferential liquid flows between blades of (a) open and (b) closed impellers. Scale of the velocity vector is the same as that in Fig. 3.

Figure 5. Bottom view of impellers of (a) open and (b) closed type rotating with gassing under higher aeration rate condition.

Figure 6. Relationships between relative power consumption and aeration number for open and closed impellers.

Figure 7. Front view of impellers of (a) open and (b) closed type rotating with gassing under lower aeration rate condition.

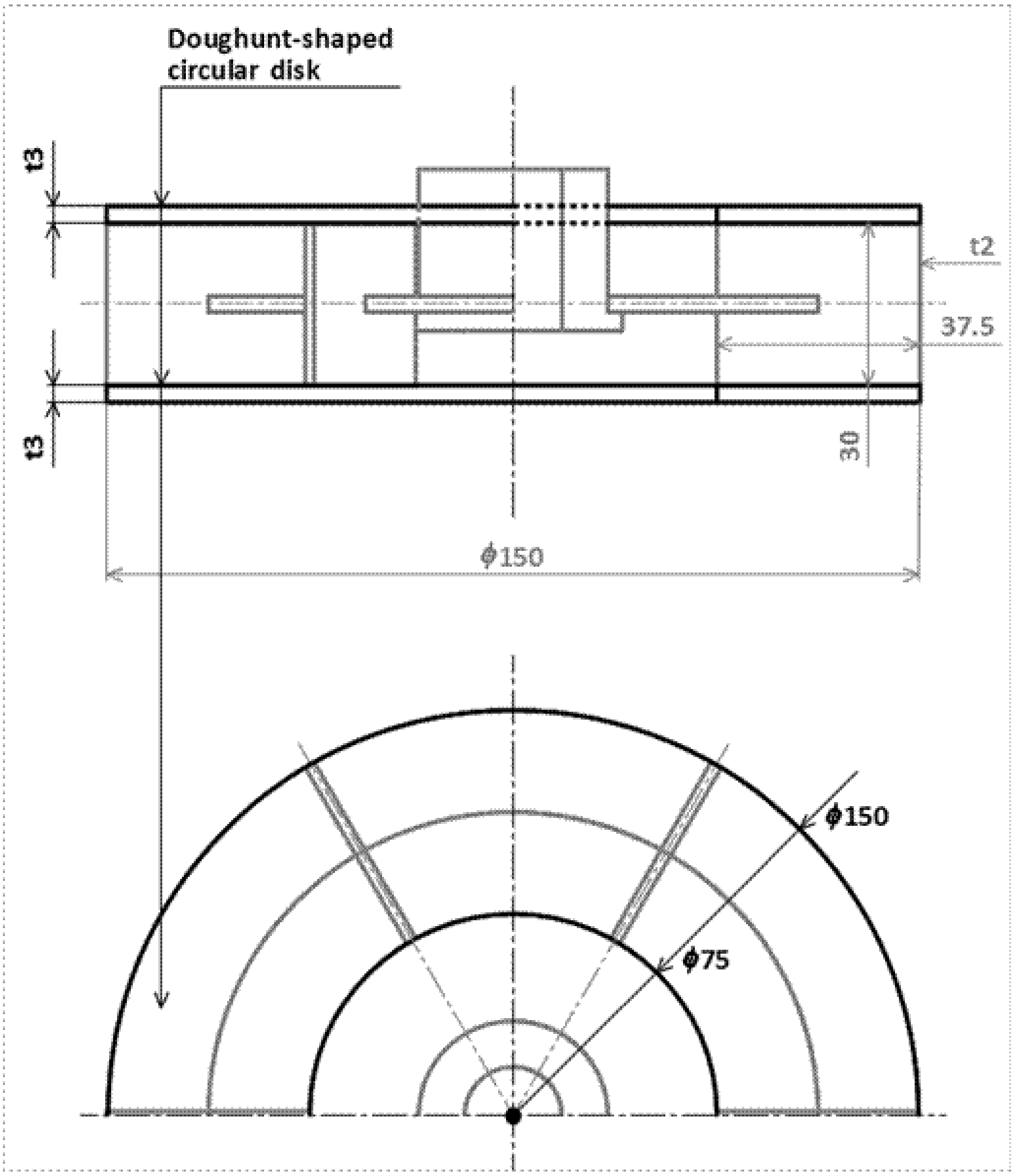

Figure 1.

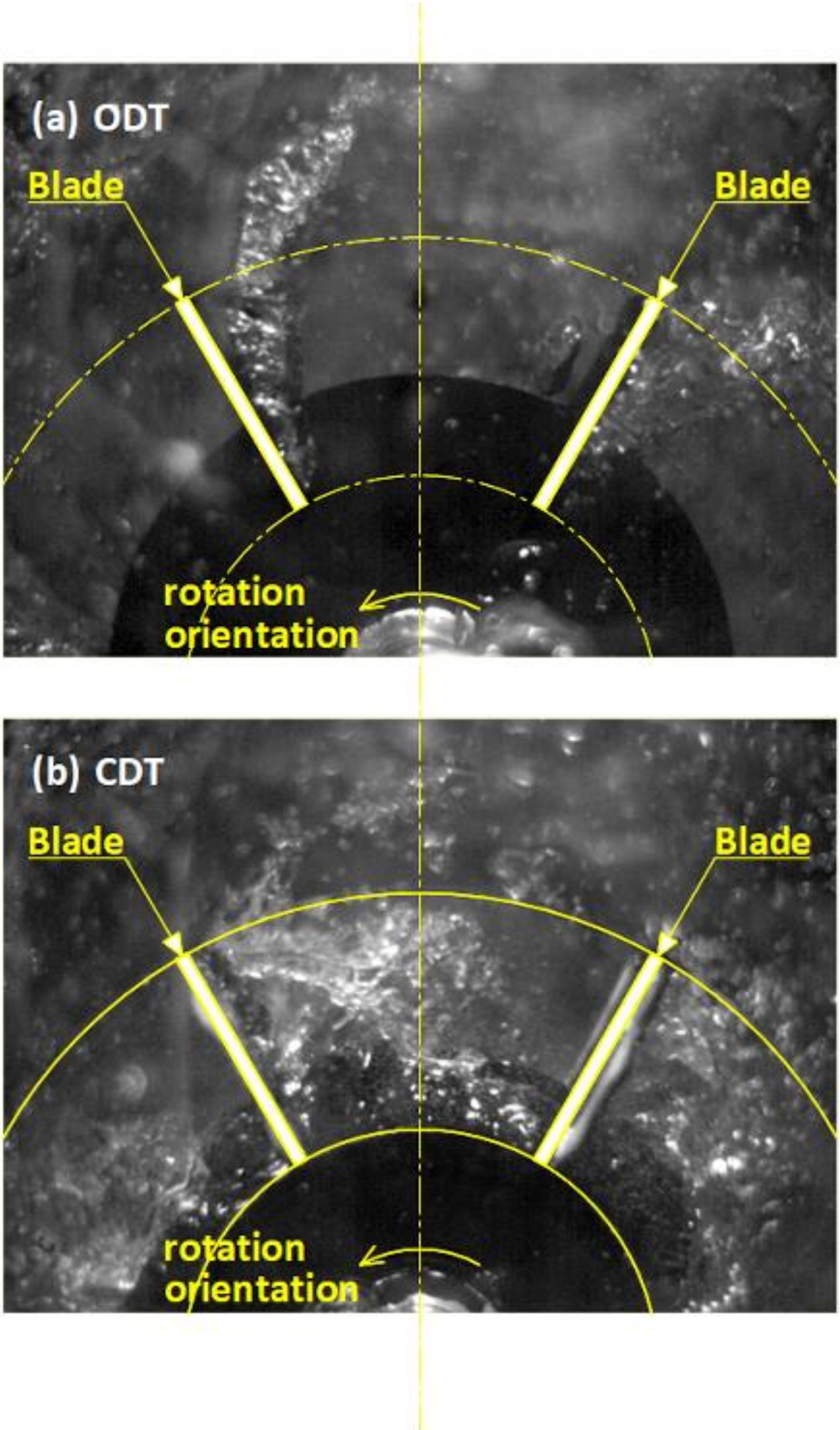
(a) ODT
Blade
Blade
rotation
orientation
(b) CDT
Blade
Blade
rotation
orientation

Figure 2.

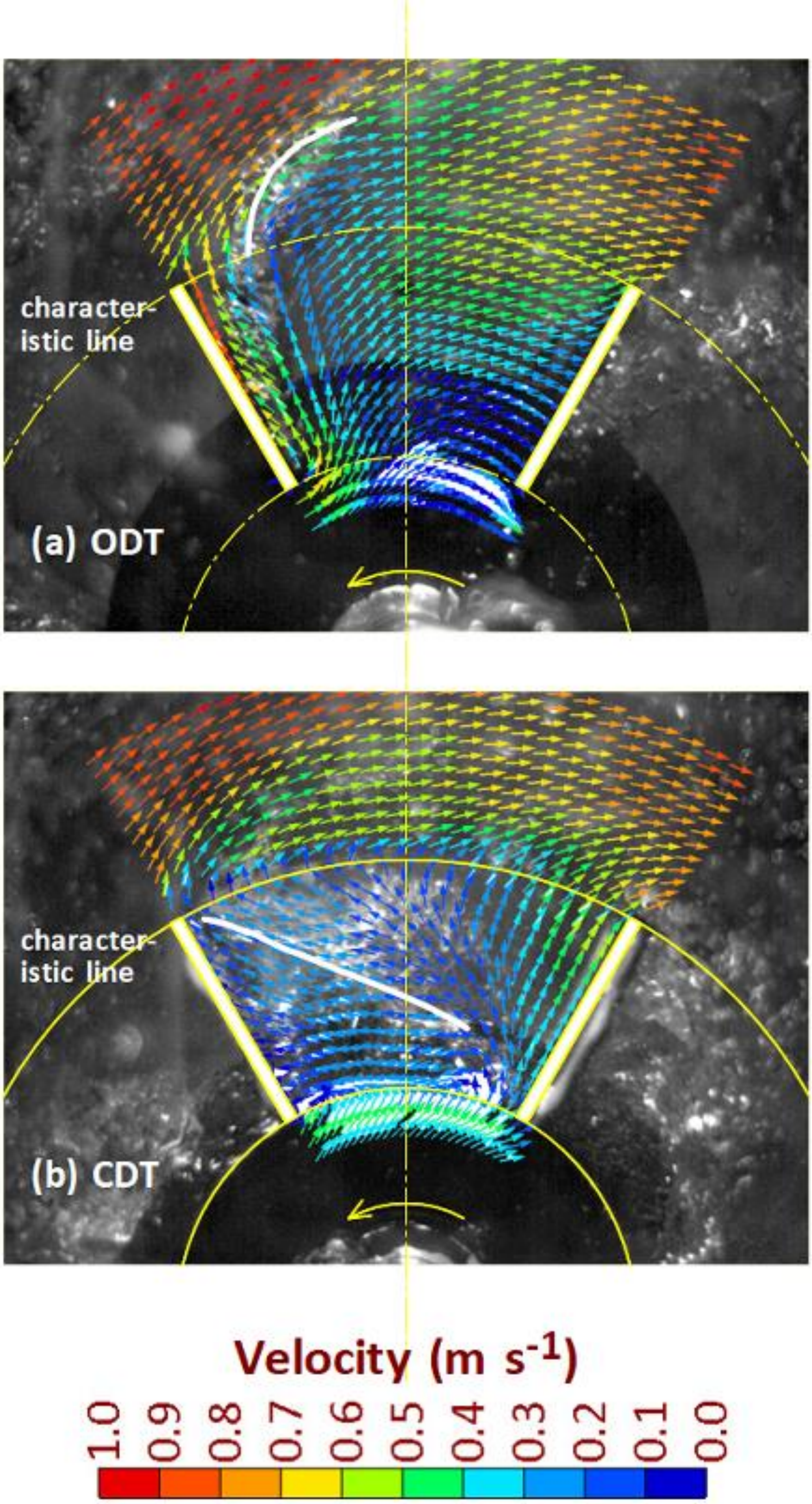
characteristic line
(a) ODT
characteristic line
(b) CDT
Velocity (m s-1)
1.0 0.9 0.8 0.7 0.6 0.5 0.4 0.3 0.2 0.1 0.0

Figure 3.

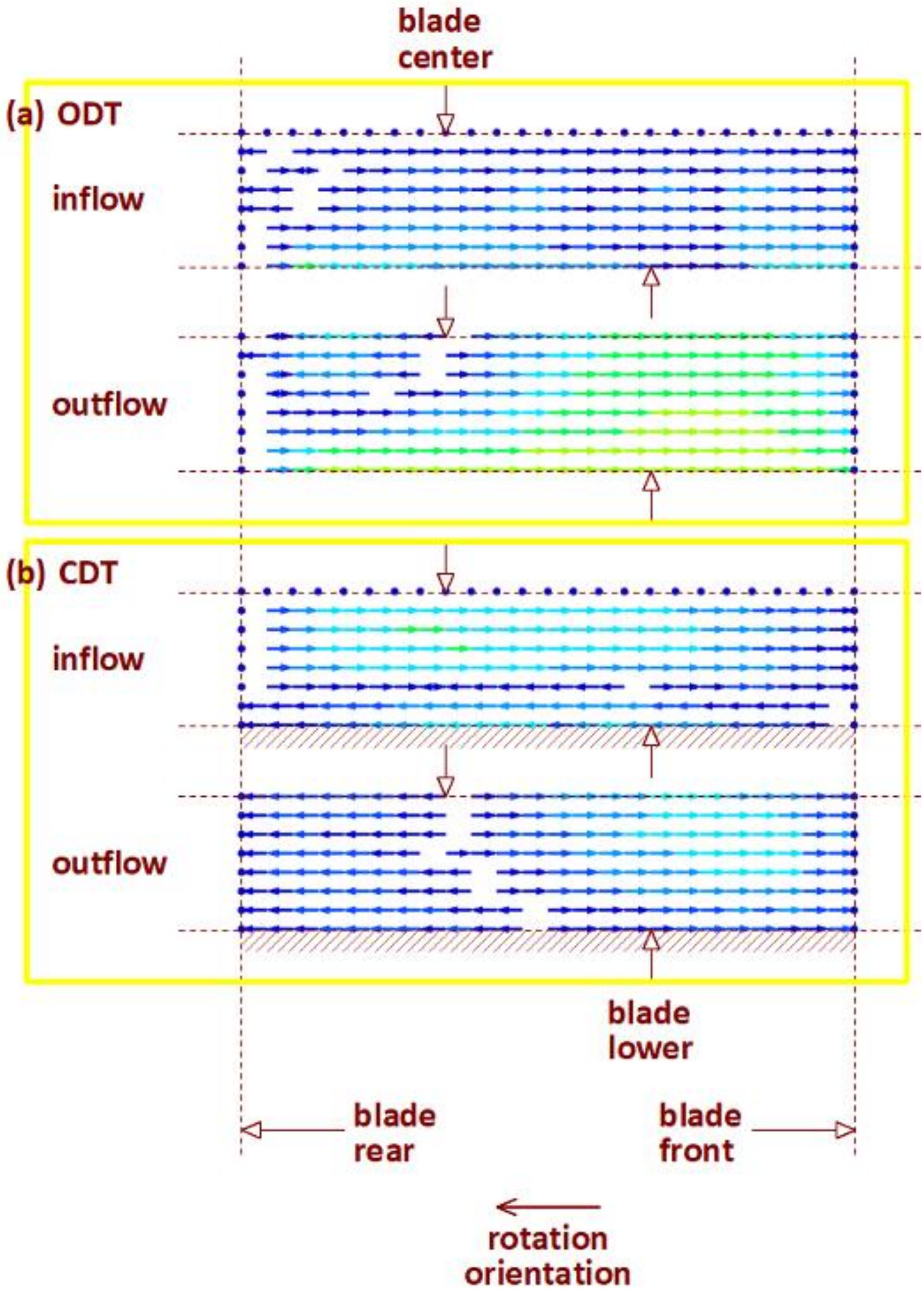
blade
center
(a) ODT
inflow
outflow
(b) CDT
inflow
outflow
blade
lower
blade
rear
blade
front
rotation
orientation

Figure 4.

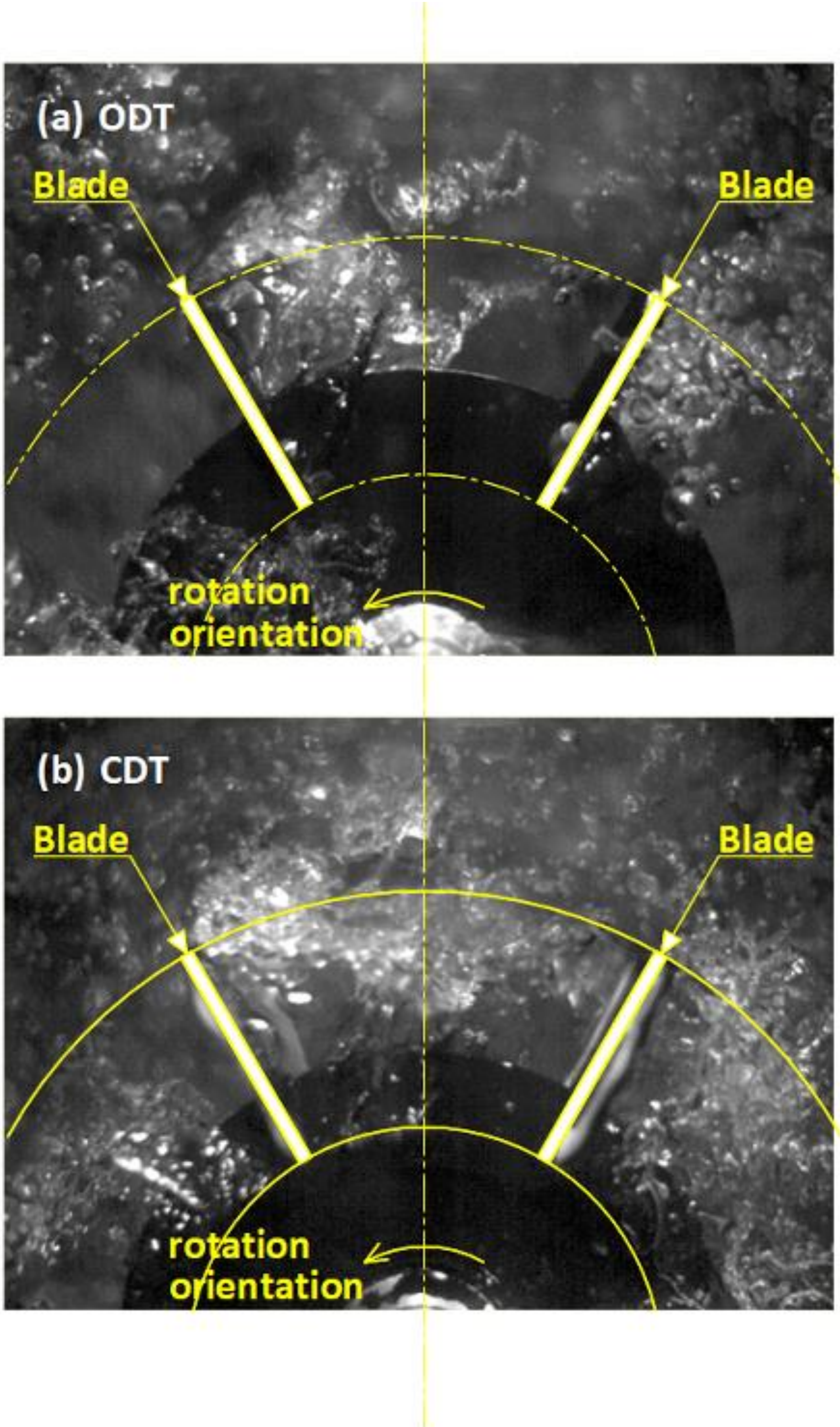
(a) ODT
Blade
Blade
rotation
orientation
(b) CDT
Blade
Blade
rotation
orientation

Figure 5.

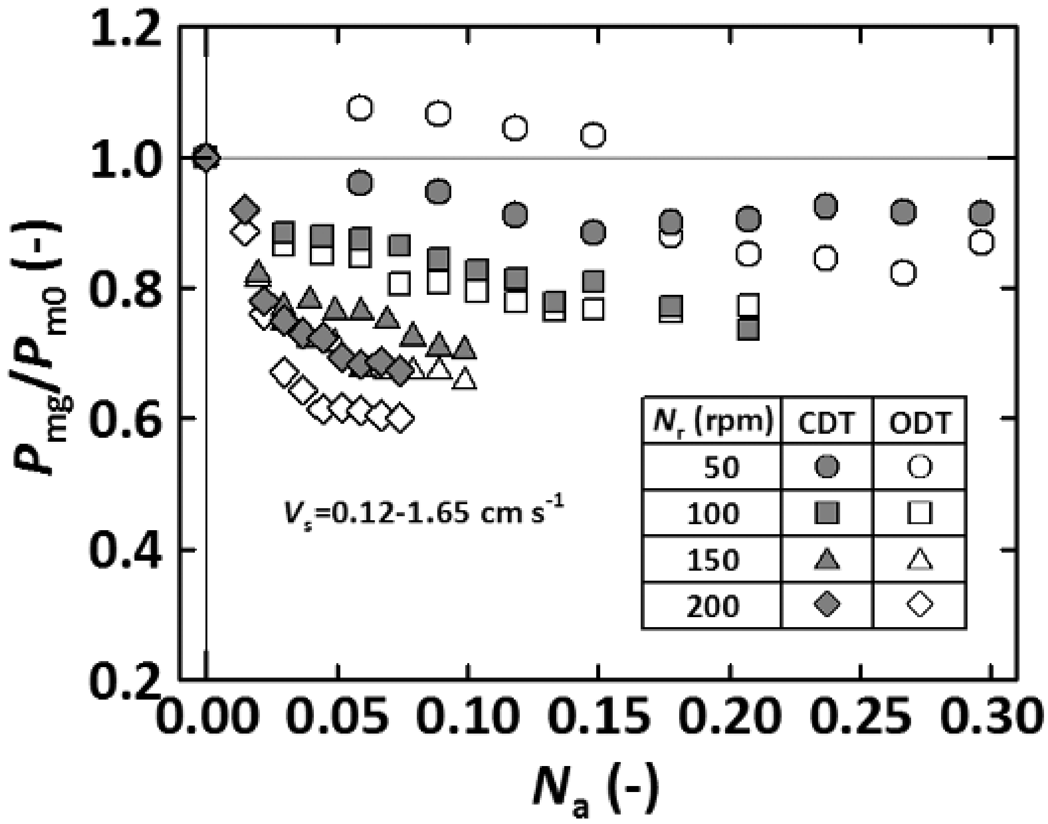

1.2
1.0
0.8
0.6
0.4
0.2
0.00
0.05
0.10
0.15
0.20
0.25
0.30
P_{mg}/P_{m0} (-)
N_a (-)
V_s=0.12-1.65 cm s^{-1}
N_r (rpm)
CDT
ODT
50
100
150
200

Figure 6.

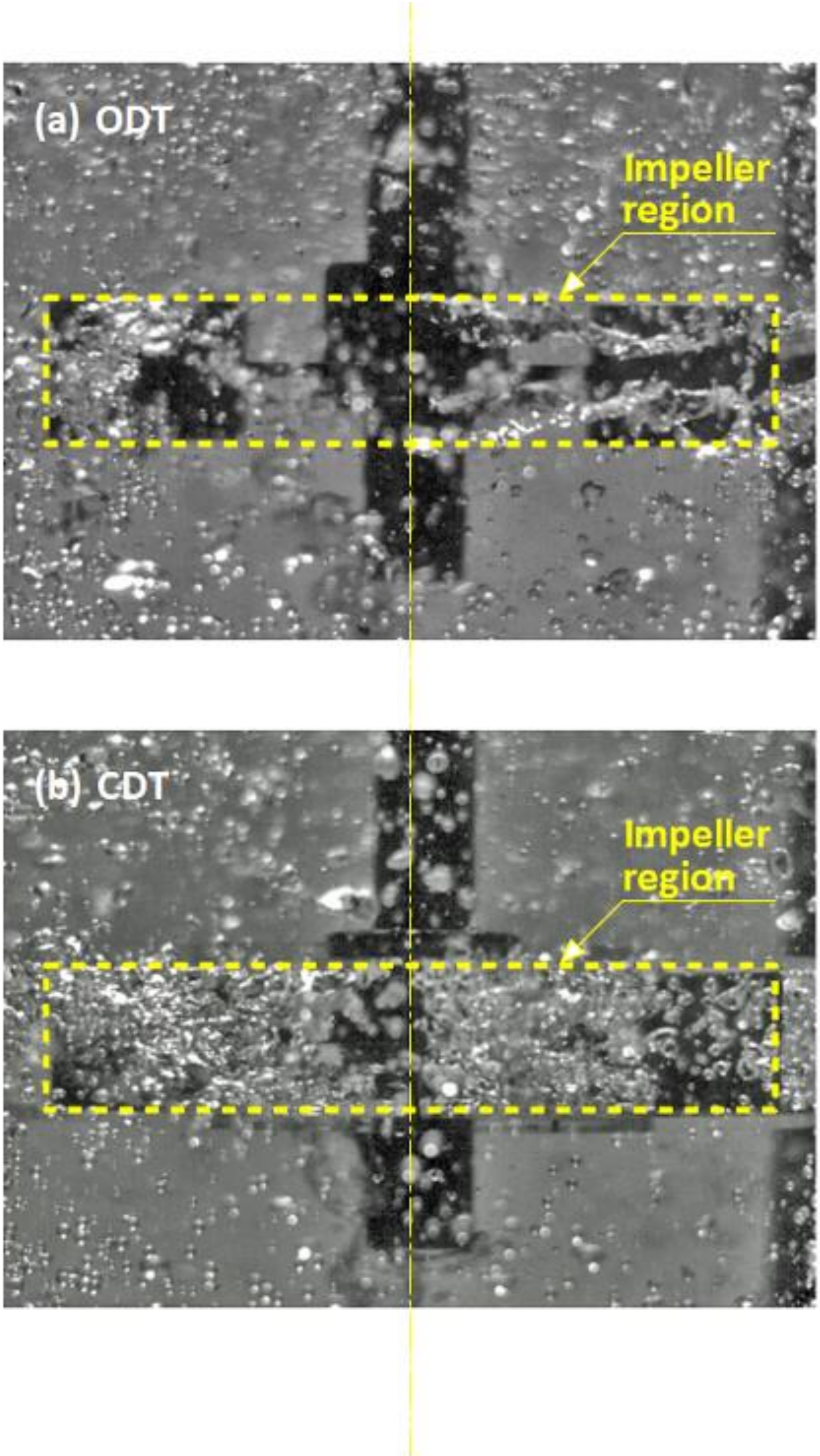

Figure 7.